Synthesis and characterization of clay-biochars produced with facile low-temperature one-step in the presence of air for adsorbing methylene blue from aqueous solution

Rui Liu[1]*, Yuncong C. Li[2], Zhimeng Zhao[1], Dandan Liu[1], Jun Ren[1] and Yang Luo[1]

[1]School of Geography and Resources, Guizhou Education University, Guiyang, China, [2]Department of Soil, Water, and Ecosystem Sciences, Tropical Research and Education Center, IFAS, University of Florida, Homestead, FL, United States

A facile and low-energy approach for biochar-supported clay preparation was developed at a low temperature (250°C) in the presence of air. A new type of engineered biochar by implanting clay particles on carbon surfaces had been successfully exploited as a low-priced adsorbent for environmental application. Two biomass feedstocks (tea and coffee wastes) were pretreated with kaolinite or montmorillonite suspension and then clay-biochars were synthesized using the facile one-step method. The adsorption performance, influencing factors, and mechanism of clay-biochars for methylene blue (MB) were investigated with adsorption experiments. The characterization results confirmed that clay exited on the biochar's surface and the adsorption results revealed that biochar-supported clay had excellent methylene blue adsorption capacities (>20 mg/g) at unadjusted solution pH and room temperature (25°C $\pm$ 1°C). Batch adsorption experiments showed that initial solution pH, ionic strength, and competing compounds affected methylene blue adsorptions. The biochar-supported clay also had a potential of recycle and reusability for methylene blue removal. The methylene blue adsorption was predominately controlled by cation exchange (with both biochar and clay) and electrostatic interaction (with biochar only) mechanisms. This study provides a simple and environmental-friendly technology for creating high-efficiency clay-biochar adsorbent for removing cationic contaminants.

KEYWORDS

biochar, biomass waste, clay, low-temperature, methylene blue, adsorption mechanism

1 Introduction

Wastewater pollution from dye industries is an important environmental and social issue, and traditional treatment methods have low efficiency in removing colored pollutants which are resistant to biological processes (Yu, 2011; Zhao et al., 2021). Compared with these conventional methods, the adsorption method is one of the best options due to its simple treatment process, more economic, and high efficiency for removing dyes from aqueous

solution (Han et al., 2016; Ngulube et al., 2017). Therefore, study on low price and high capacity adsorbents for dyes is much more attractive.

Kaolinite (KLN) and montmorillonite (MMT) are common clays which usually exhibit excellent adsorption ability due to high cation exchange capacity (CEC), thus, both clays can effectively remove many kinds of cationic pollutants (Kaya, 2004; Zhuang and Yu, 2022). However, KLN an MMT are unsuitable to be applied in water treatment facilities directly because they are difficult for application, dispersion, and recovery due to very fine particles (Yao et al., 2014).

Biochar, an emerging carbon material stemmed from different low-priced biomass residuals, has been recommended as an environmental-friendly adsorbent to adsorb pollutants and as a matrix to fix the tiny particles since it has an excellent porous structure, surface area, and plenty of adsorption sites. In order to boost the adsorption performance of pristine biochar, much attention has been given to developing engineering technologies to produce carbon-based adsorbents with promoted functions for pollutants removal, such as surface modification (Xue et al., 2012; Sizmur et al., 2017; Liu et al., 2021). Currently, most biochars are created by conventional technologies, for example, slow pyrolysis, hydrothermal carbonization (Mohan et al., 2014; Gong et al., 2022). One of the drawbacks of these technologies is high temperature process, which consumes a large quantity of electricity, and a production rate is relatively low. It is also impossible to produce on a large scale. Another disadvantage is to provide the oxygen-limited condition, which means that a closed reactor always needs to be used. Very few studies regarding low temperature (150°C–300°C) synthesis methods have been reported to date, particularly in the presence of air. Low-temperature and the presence of air make the biochar production process much more attractive and have better yields (Simsir et al., 2007).

Methylene blue (MB), a typical cationic dye, is a common pollutant in wastewater from paper and textile factories. The presence of MB can lead to detrimental impacts on aquatic life and even on human beings (Iriarte-Velasco et al., 2011; Yan et al., 2011). A clay-biochar (MMT modification) prepared by conventional technology has an excellent MB adsorption performance and a maximum adsorption capacity of more than 11 mg/g (Yao et al., 2014). Meanwhile, previous studies have reported that biochars synthesized through a facile one-step technology at low temperatures in the presence of air with 85% H_3PO_4 enhances the adsorption capacities of MB and other cations (Zhao et al., 2018; Ge et al., 2020). Combining these cases and the advantages of clays and biochars mentioned above, we hypothesize that clay-biochar materials with enhanced value and functions for MB removal may also be produced at low temperatures in the presence of air. This innovative technology should lead to simple, environmental-friendly, and high-yield biochar production.

This work aimed to develop a simple and environmental-friendly technology for preparing clay-biochar materials to adsorb MB from an aqueous solution. In this work, the low-priced clay-biochar adsorbents were created from beverage byproducts (i.e., tea and coffee wastes) pretreated with clay (KLN and MMT) suspension through a facile one-step technology at low temperature (250°C) in the presence of air and their adsorption capacity of MB were evaluated. The properties of these biochars were

characterized. Also, the influencing factors [initial solution pH, ionic strength (IS), competing compounds] and the mechanisms of MB adsorption were examined.

2 Materials and methods

KLN and MMT were purchased from Tianjin Chemical Works Co. Ltd (Tianjin, China). Tea waste (TW) and coffee waste (CW) were obtained from residues of green tea and coffee from Lipton Co. Ltd (Hangzhou, China) and Illy Coffee Co. Ltd (Trieste, Italy), respectively. All other reagents used in this work including MB, NaOH, 65%HNO₃, NaCl, humic acid (HA), NH₄Cl, MgCl₂, and CaCl₂ were obtained from Shanghai Chemical Works Co. Ltd (Shanghai, China).

2.1 Biochar production

Before pyrolysis, two biomass feedstocks (TW and CW) were first modified with KLN and MMT, respectively. The procedure of clay-treated biomass feedstocks was based on Yao et al.s literature (Yao et al., 2014). Then, the biomass feedstocks with clay treatment were carbonized in an oven in the presence of air for 2 h at 250°C. TW and CW were also carbonized directly to prepare biochars and served as pristine biochars in the same pyrolysis method. All biochar samples were sieved through 0.5–0.25 mm, washed with DI water until the pH was neutral, oven dried (80°C), and sealed in a vaccum desicator for further examine. The resulting biochar-supported clay and pristine biochar samples were labeled as KLN-TWBC (kaolinite modified tea waste biochar), MMT-TWBC (montmorillonite modified tea waste biochar), KLN-CWBC (kaolinite modified coffee waste biochar), MMT-CWBC (montmorillonite modified coffee waste biochar), TWBC (tea waste biochar) and CWBC (coffee waste biochar).

2.2 Characterizations

For all six biochar samples, the physicochemical properties including surface area, organic and major inorganic elements, and production rate, were determined in this work. The N₂ surface areas of these biochars were measured using ASAP2460 surface area analyzer (Micromeritics, United States) and were calculated using BET method. Organic elements (such as C, H, and N) analyses were obtained using an Elemental Analyzer (Perkin Elemer 2400, United States). The main inorganic elements of the six biochars were measured by acid digestion of the samples followed by inductively-coupled plasma atomic emission spectroscopy (ICP-OES, Horiba Ultima Expert, France) analysis. Oxygen level was tested by a mass balance presuming the weight of all analyzed elements equals 1. The different weights between feedstocks and biochars were measured to obtain the production rates. In addition, the morphology and composition of elements of KLN-TWBC and MMT-TWBC's surface were analyzed using a scanning electron microscope equipped with an energy dispersive X-ray spectroscopy (SEM, Tescan Mira LMS, Czech; EDX, Xford 30, Britain).

2.3 Adsorption experiments

2.3.1 Methylene blue adsorption ability

The MB adsorptions ability of KLN-TWBC, MMT-TWBC, KLN-CWBC, and MMT-CWBC were evaluated using 100 mL digestion vessels with a 1: 500 biochar/solution ratio (0.05 g biochar in 25 mL solution) at room temperature ($25°C ± 0.5°C$). The MB concentration in solution was 20 and 500 mg/L, respectively. After shaking at 120 rpm for 48 h (sufficient to reach adsorption equilibrium), the mixtures were filtered through 0.22 um pore size nylon membrane filters (cellulose nylon membrane), and the adsorbed MB concentrations was measured by a UV-722 spectrometer (Kejie, China) at λ_{max} of 662 nm. TWBC and CWBC served as a control in the experiment where the operation procedure was the same as that of biochars with KLN and MMT modification.

2.3.2 Influence factors of methylene blue adsorption ability

The effect of initial solution pH on MB adsorption was researched over a range of 2–11 (i.e., 2.0, 4.0, 6.8, 9.0, and 11.0). Varying initial pH with MB concentration of 20 mg/L was adjusted by adding 0.01 mol/L $NaOH/HNO_3$ to 20 mg/L MB solutions into vessels. Also, the effect of IS was tested by adding NaCl into 20 mg/L MB solutions, and the concentration of NaCl ranged from 0.001 to 0.1 mol/L. In addition, the effects of competing compounds were investigated through an adsorption test for common coexisting cations (i.e., Na^+, Mg^{2+}, Ca^{2+} and NH_4^+) or organic matter (HA). Based on their common concentrations in wastewater (Liu et al., 2018), 157 mg/L Na^+(NaCl, 6.84 mmol/L), 101 mg/L Mg^{2+} ($MgCl_2$, 4.21 mmol/L), 144 mg/L Ca^{2+} ($CaCl_2$, 3.60 mmol/L), 67 mg/L NH_4^+ (NH_4Cl, 3.74 mmol/L), 2.0 mg/L HA, or the mixture of NaCl, NH_4Cl and HA was used in this work. Other procedures of the experiment were the same as the one described above.

2.3.3 Adsorption kinetics and isotherm

20 mg/L MB solution was prepared, and time intervals of 0.5, 1, 4, 8, 16, 24, 48, and 72 h were selected for the kinetics study. The isotherm study was conducted with various MB solution concentrations varying from 10 to 500 mg/L for 48 h. The initial solution pH was about 6.80 ± 0.10 which was an unadjusted pH with an initial concentration of 20 mg/L MB, and the pH value was used in all solutions in the adsorption experiments.

2.3.3.1 Adsorption kinetics model

In addition to the commonly used pseudo-first-order and pseudo-second-order models, the Elovich model and intraparticle diffusion model were examined. On the basis of mononuclear and binuclear adsorption, the kinetics of the solid-liquid system is described by first- and second- order. The models of Elovich and intraparticle diffusion describe the contribution of desorption and a diffusion process for adsorbate on the adsorbent, respectively.

$$\frac{dQ_t}{dt} = k_1 (Q_e - Q_t) \quad \text{first} - \text{order} \tag{1}$$

$$\frac{dQ_t}{dt} = k_2 (Q_e - Q_t)^2 \quad \text{second} - \text{order} \tag{2}$$

$$\frac{dQ_t}{dt} = a\exp(-\beta Q_t) \quad \text{Elovich} \tag{3}$$

$$q_t = k_i t^{1/2} + C_i \quad \text{intraparticle diffusion} \tag{4}$$

Where Q_t and Q_e represent the amount of MB at time t and equilibrium, respectively (mg/g), and k_1 and k_2 represent the first-order, second-order apparent adsorption rate constants [h^{-1} and g (mg h)$^{-1}$], respectively. k_i represents the intraparticle diffusion constant [mg/(g $h^{1/2}$)]. Also, a represents the initial adsorption rate [mg/(g h)], and ß represents the desorption constant (g/mg). In addition, C_i represents the intercept of the intraparticle diffusion, and i represents the diffusion phase.

2.3.3.2 Adsorption isotherm model

Langmuir, Freundlich, Langmuir-Freundlich, and Redlich-Peterson, four common models, were used to fit the isotherm experimental data to explore how the adsorbate is distributed from the liquid to the solid phases under an equilibrium condition.

$$Q_e = \frac{KQC_e}{1 + KCe} \quad \text{Langmuir} \tag{5}$$

$$Q_e = K_f C_e^n \quad \text{Freundlich} \tag{6}$$

$$Q_e = \frac{K_{lf}QC_e^n}{1 + K_{lf}C_e^n} \quad \text{Langmuir} - \text{Freundlich} \tag{7}$$

$$Q_e = \frac{K_r C_e}{1 + aC_e^n} \quad \text{Redlich} - \text{Peterson} \tag{8}$$

Where Q represents the maximum capacity (mg/g); C_e represents the equilibrium solution concentration of MB (mg/L); K, K_f, K_{lf} and K_r represent the Langmuir bonding term related to interaction energies (L/mg), the Freundlich affinity coefficient (mg$^{(1-n)}$ L^n), Langmuir-Freundlich affinity parameter (L^n/mg^n), and the Redlich-Peterson isotherm constants (L/g), respectively; n represents the Freundlich linearity constant, and a represents the Redlich-Peterson isotherm constant (L^n/mg^n). Monolayer adsorption onto a homogeneous surface is described by the Langmuir model. In contrast, the other three models, as empirical or semiempirical models, usually describe heterogeneous adsorption processes.

2.4 Regeneration of biochar-supported clay

Regeneration studies were conducted using KLN-TWBC and MMT-TWBC with MB saturation, which were obtained from isotherm experiments after discarding MB solution. The regeneration experiment was assessed *via* four successive adsorption-desorption tests, and 0.5 mol/L KCl was used as the desorption agent. The specific steps can be referred to in the previous literature (Liu R. et al., 2019). Considering the adsorption of MB on clay is chiefly through cation exchange, using KCl solution to desorb MB would reveal not only the potential of cycle performance but also investigate the effect of KLN and MMT on the adsorption of MB onto the two composite adsorbents (Yao et al., 2014).

2.5 Statistical analysis

All adsorption experiments were carried out in triplicate, and the average data were used. Differences between the means were

TABLE 1 Surface area, production rate and elemental analysis of TWBC, KLN-TWBC and MMT-TWBC.

Sample id	Surface area m²/g	Yield %	Mass based %[b]														
			C	H	N	O	Na	Mg	Ca	Fe	Al	P	Pb	Mn	Zn	Cu	Cd
TWBC	358.1	55.30	59.90	4.38	0.30	24.13	0.04	0.22	0.89	0.06	0.21	0.01	nd[a]	nd	nd	nd	nd
CWBC	325.4	56.94	54.72	4.13	0.46	20.50	nd	0.17	0.65	0.02	0.13	0.01	nd	nd	0.01	nd	nd
KLN-TWBC	349.9	57.81	61.95	3.90	0.28	27.88	0.02	0.20	0.93	0.19	0.57	0.01	nd	nd	nd	nd	nd
MMT-TWBC	336.5	56.66	63.31	3.74	0.21	25.39	0.06	0.17	0.87	0.19	0.69	0.01	nd	nd	nd	nd	nd
KLN-CWBC	313.8	56.07	52.51	3.76	0.37	23.99	0.02	0.15	0.59	0.10	0.37	0.02	nd	nd	nd	nd	nd
MMT-CWBC	303.2	57.52	53.33	3.93	0.41	22.76	0.02	0.21	0.67	0.12	0.44	0.01	nd	nd	nd	nd	nd

[a]Below the detection limit.
[b]The data was the average of the three replicates.
TWBC, tea waste biochar; CWBC, coffee waste biochar; KLN-TWBC, kaolinite modified tea waste biochar; MMT-TWBC, montmorillonite modified tea waste biochar; KLN-CWBC, kaolinite modified coffee waste biochar; MMT-CWBC, montmorillonite modified coffee waste biochar.

statistically analyzed with one-way ANOVA followed by Tukey's HSD test at a significance level of $p < 0.05$. Error bars were used to represent standard deviations. Origin 8.5 software was used to conduct all statistical analyses and perform kinetics and isotherm figures. Excel 2020 software was used to perform other figures.

3 Results and discussion

3.1 Properties of biochars

3.1.1 Production rate, elemental analysis, and surface area

Previous studies have suggested that the production rates of biochars synthesized through conventional technologies are between 25% and 45%, and the yield is generally controlled by temperature and raw materials (Mohan et al., 2014; Yang J. H. et al., 2021). In this work, the yields of six biochars ranged from 55.30% to 57.81% (Table 1), which is higher than that of biochars prepared using conventional technologies. There was no noticeable difference in yields among biochars with and without clay treatment, indicating that production rates of biochars can be increased through this facile one-step technology. Elemental analysis of carbon (C), hydrogen (H), and nitrogen (N) showed that all six biochar samples produced were rich with carbon varying from 52.51% to 63.31% (Table 1), which indicated that the facile one-step technology had created a carbon-based adsorbent (Yao et al., 2013a; Meng et al., 2022). The C contents of the TWBC-based biochars were higher than that of CWBC-based biochars, and clay-TWBCs and clay-CWBCs were similar to their feedstocks instead of clay types, indicating that C contents of biochars were not alerted by clay treatment and the feedstock category was the key factor. It is consistent with the previous studies, as Basta et al. (2009 and 2011) reported that some chemical components (i.e., lignin and cellulose levels) of the feedstocks, may govern the yield and quality of bicohars. In addition to C, H and N are also major elements of biochars, some of which exist in the form of surface functional groups (Mohan et al., 2014; Liu M. et al., 2019; Chen et al., 2019; Gong et al., 2022). Compositions of H and N in six biochar samples ranged from 3.74% to 4.38% and 0.21%–0.46%, respectively. Compared with conventional bichars (Supplementary Table S1), there was a significant increase in the O contents of the samples in this work, which is probably due to the participation of much more oxygen during synthesis in the presence of air (Mohan et al., 2014; Yan et al., 2018; Ge et al., 2020). Also, we have seen that the O contents of biochars from the same feedstock category were comparable with each other, however, that of KLN-biochars was slightly higher, which may be attributed to the high O content of KLN (Murray, 1991). The O contents of two feedstocks followed the order of TWBC > CWBC, which reflected that O level in biochar mainly depends on the feedstock category, while clay treatment only mildly alters it.

In Table 1, the main inorganic element analysis indicated that KLN and MMT modification significantly increased the biochar's Al content, a major element of both clays. Additionally, the Fe contents of clay-TWBCs and clay-CWBCs were higher than that of TWBC and CWBC, which can be attributed to changing amounts of Fe in both clays. The two reasons could be explained as (1) Fe is a substitute in MMT, since Fe (III) can exchanged with Al (III) (Wang et al., 1996); and (2) KLN can hold Fe into its octahedral sheet (Yao et al., 2014). The dramatically
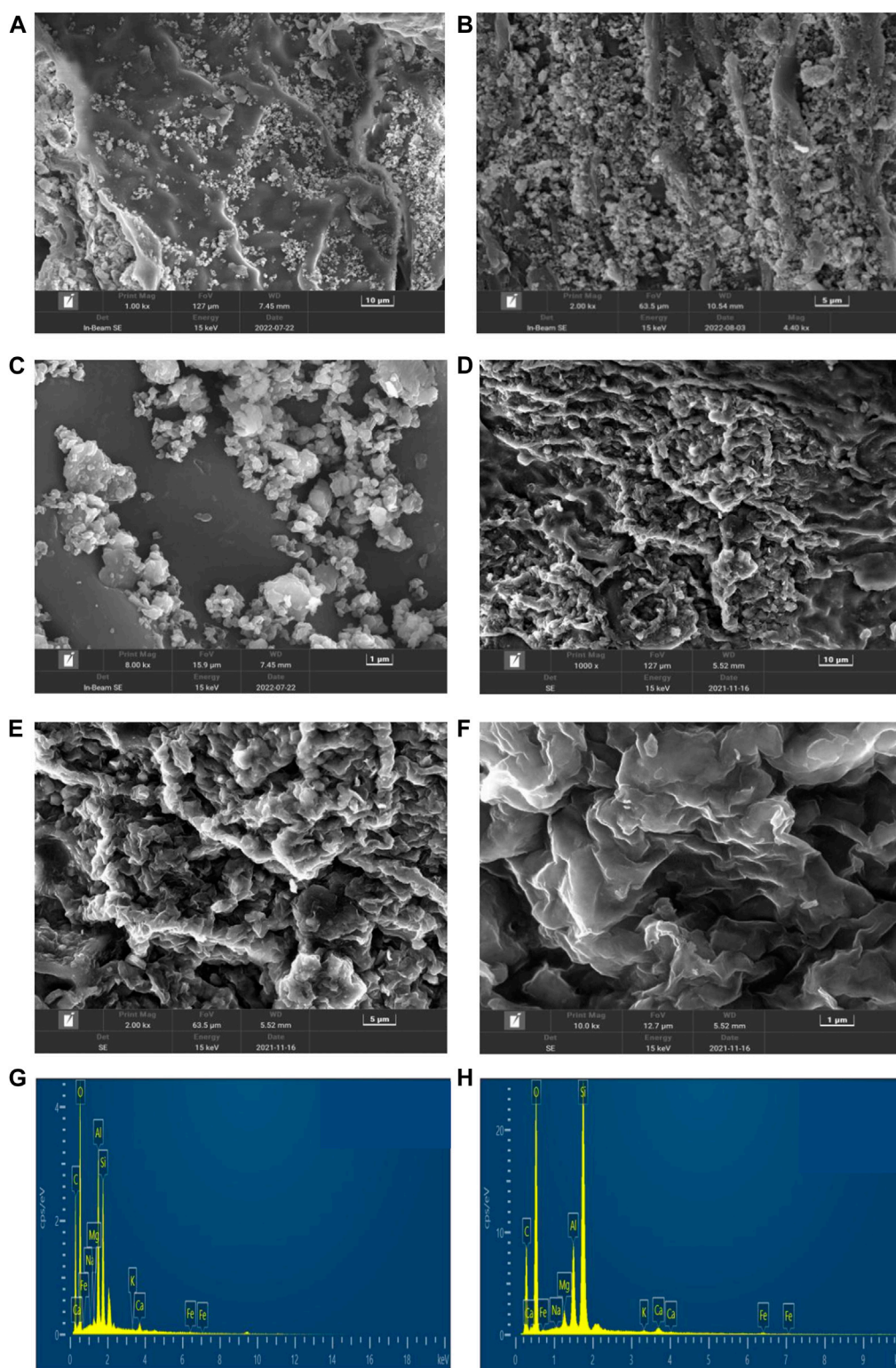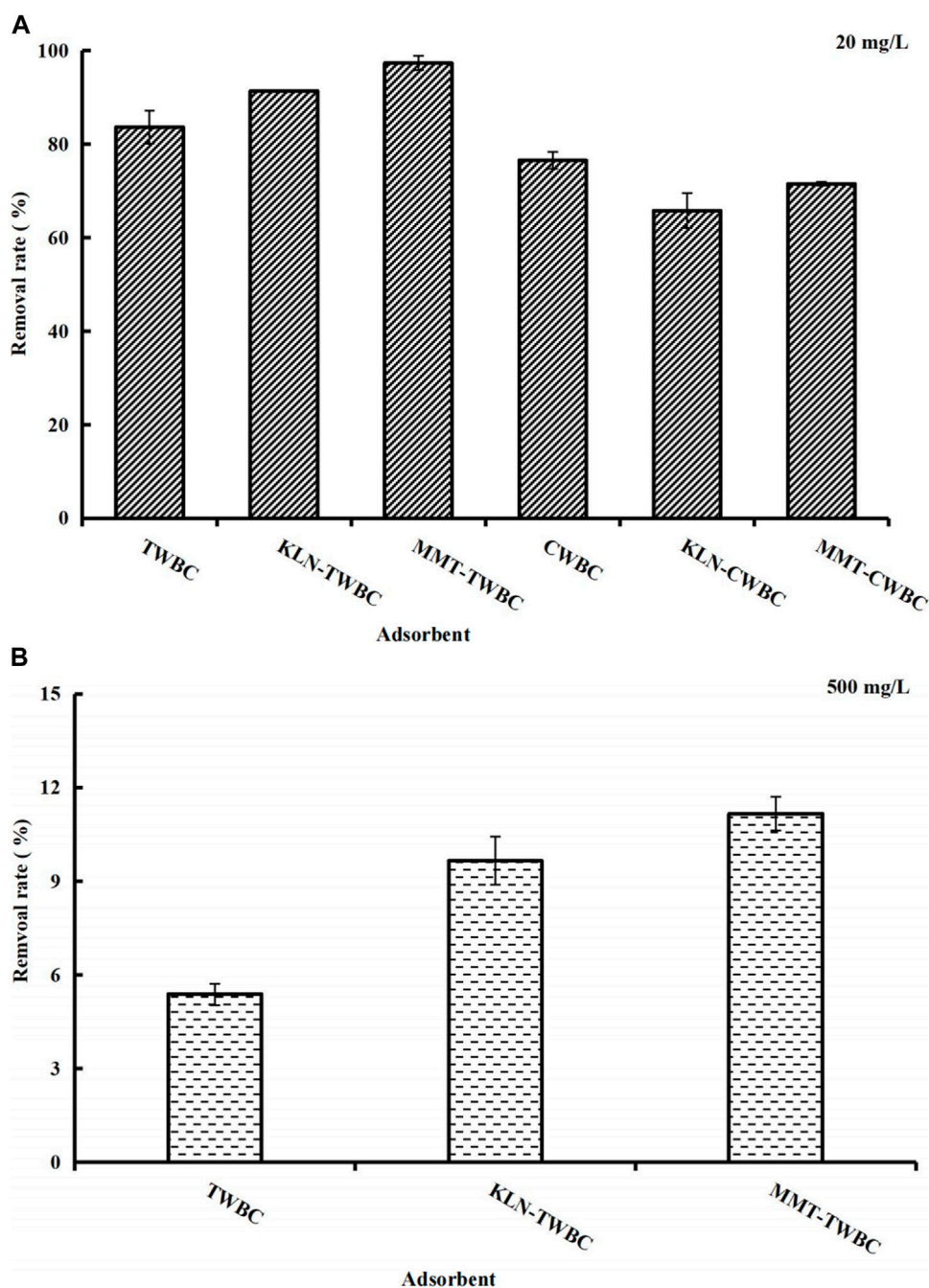
FIGURE 1
SEM image **(A–F)** and EDX spectrum **(G, H)** of the two biochar samples: **(A)** KLN-TWBC, 1,000×: **(B)** KLN-TWBC, 2000×; **(C)** KLN-TWBC, 8,000×, **(D)** MMT-TWBC, 1,000×: **(E)** MMT-TWBC, 2000×; **(F)** MMT-TWBC, 100,00×. The EDS spectra **(G, H)** were obtained at the same location as shown in the SEM image **(C, F)**. KLN-TWBC, kaolinite modified tea waste biochar, and MMT-TWBC, montmorillonite modified tea waste biochar.

increased Al and Fe contents of clay-biochars revealed that both clays were successfully implanted into the biochars. Other elements levels were relatively low and similar to each other.

Six biochars exhibited large surface areas following the order of TWBC > KLN-TWBC > MMT-TWBC > CWBC > KLN-CWBC > MMT-CWBC. The reduced surface area of raw material treated with
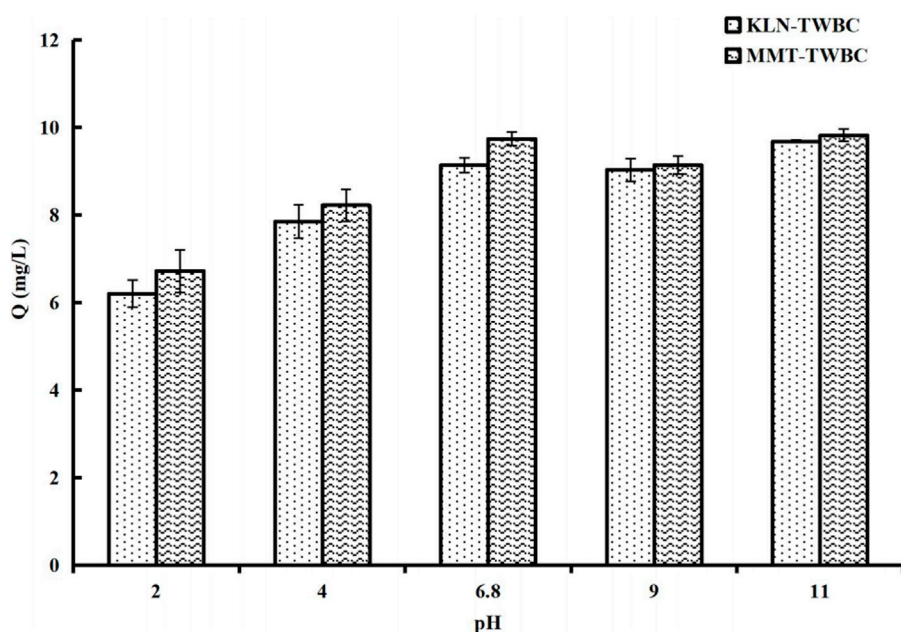
FIGURE 2
Removal rates of **(A)** low initial concentration (20 mg/L) MB by TWBC, KLN-TWBC, MMT-TWBC, CWBC, KLN-CWBC, MMT-CWBC, and **(B)** high initial concentration (500 mg/L) MB by TWBC, KLN-TWBC, MMT-TWBC (Contact time 48 h, temperature 25°C $\pm$ 0.5°C, adsorbent dose 2 g/L, MB solution 25 mL, and pH 6.80 $\pm$ 0.10). TWBC, tea waste biochar; CWBC, coffee waste biochar; KLN-TWBC, kaolinite modified tea waste biochar; MMT-TWBC, montmorillonite modified tea waste biochar; KLN-CWBC, kaolinite modified coffee waste biochar, and MMT-CWBC, montmorillonite modified coffee waste biochar.

clays especially with MMT, probably should be attributed to MMT quickly covering/clogging the pores on the biochars due to its smaller size than that of KLN.

3.1.2 Surface morphology

To further confirm that the clay particles were successfully implanted on the surface of TWBC, KLN-TWBC and MMT-TWBC

were analyzed by SEM-EDX. The image (Figures 1A, B, D, E) showed that there were many tiny particles distributed onto the surface of TWBC, and the EDX spectrum of these particles showed high peaks for typical elemental compositions of clay minerals (aluminum, iron, calcium, magnesium, silicon, and sodium) (Figures 1G, H). After zooming in at ×8,000 magnification, TWBC covered with KLN and MMT can be seen. However, the coverage on the biochar's surface varied

FIGURE 3
Effect of pH on MB adsorption for KLN-TWBC and MMT-TWBC (Initial MB concentration of 20 mg/L, contact time 48 h, temperature 25°C $\pm$ 0.5°C, adsorbent dose 2 g/L, and MB solution 25 mL). KLN-TWBC, kaolinite modified tea waste biochar; MMT-TWBC, montmorillonite modified tea waste biochar. Error bars represent the standard deviations of triplicate samples.

with KLN and MMT. KLN existed on the surface of TWBC as particles, while MMT can be seen as a thin film (Figures 1C, F), which also contributes to the reason that MMT-TWBC had a lower surface area but relatively higher MB adsorption ability than that of KLN-TWBC.

3.2 Methylene blue adsorption ability and influence factors

3.2.1 Adsorption ability

The MB adsorption ability was investigated for each of all six biochars and the results showed that TWBC and CWBC had more than 50% MB removal rate, revealing that TW and CW might be good raw materials for the production of biochar-based adsorbents prepared through the facile one-step technology (Figure 2). After modification with KLN and MMT, MB removal rates varied with different feedstocks. The presence of clays increased MB adsorption of TWBC by 7.73% for KLN and 13.7% for MMT. Conversely, it slightly decreased the adsorption of MB onto clay-CWBCs, suggesting that it is unsuitable to apply clay-CWBC materials to remove MB. Further studies are required to seek the reason for lower MB adsorption performance and to optimize its ability. To further test the MB adsorption ability of KLN-TWBC and MMT-TWBC, a higher MB concentration was used in the adsorption experiment. The result demonstrated that both clay-TWBCs had higher MB removal rates than TWBC, and the adsorption ability was MMT-TWBC > KLN-TWBC > TWBC, which could be attributed to the presence of both clays. Meanwhile, the result is consistent with previous studies that clays (i.e., KLN and MMT) generally has excellent ion exchange ability for many kinds of cationic pollutants, such as MB (Ma et al., 2004; Gurses et al., 2006; Klika et al., 2011). Because of best MB adsorption

ability, both clay-TWBCs were selected for additional investigation, including influence factors for MB adsorption and identification of adsorption mechanisms.

3.2.2 Effect of initial pH

The relationship between the initial pH and MB adsorption ability of KLN-TWBC and MMT-TWBC is shown in Figure 3. With ranging pH from 2.0 to 6.8, the adsorption of MB onto MMT-TWBC was higher than that onto KLN-TWBC, and a similar change trend occurred in both clay-biochars. The MB adsorption was lowest when pH equaled 2.0. When pH was enhanced from 2.0 to 6.8, the adsorption of MB was promoted from 6.20 to 9.14 mg/L for KLN-TWBC and from 6.72 to 9.74 mg/L for MMT-TWBC. Further increasing pH from 6.8 to 11.0; however, there was no distinct effect of changing pH on the adsorption of MB onto both clay-biochars. The varying MB adsorption ability of KLN-TWBC and MMT-TWBC, depending on the initial pH, can be ascribed to the presence of H^+ in the solution (Liu et al., 2018; Zhao et al., 2018). At the conditions of lower initial pH, both clay-biochars had low adsorption ability, which can be attributed to the protonation of H^+ from the solution decreasing the active adsorption sites. As the pH value is over 6.80, more adsorption sites on the biochar's surface can be served for MB adsorption because of the deprotonation reactions with reduced H^+. Consequently, both clay-biochars exhibited a steady and excellent adsorption ability for MB, especially at neutral and alkali pH conditions.

3.2.3 Effect of ionic strength and competing compounds

In addition to pH, other ions can possibly interfere with the adsorption ability of MB. To assess the resilience to counter ions
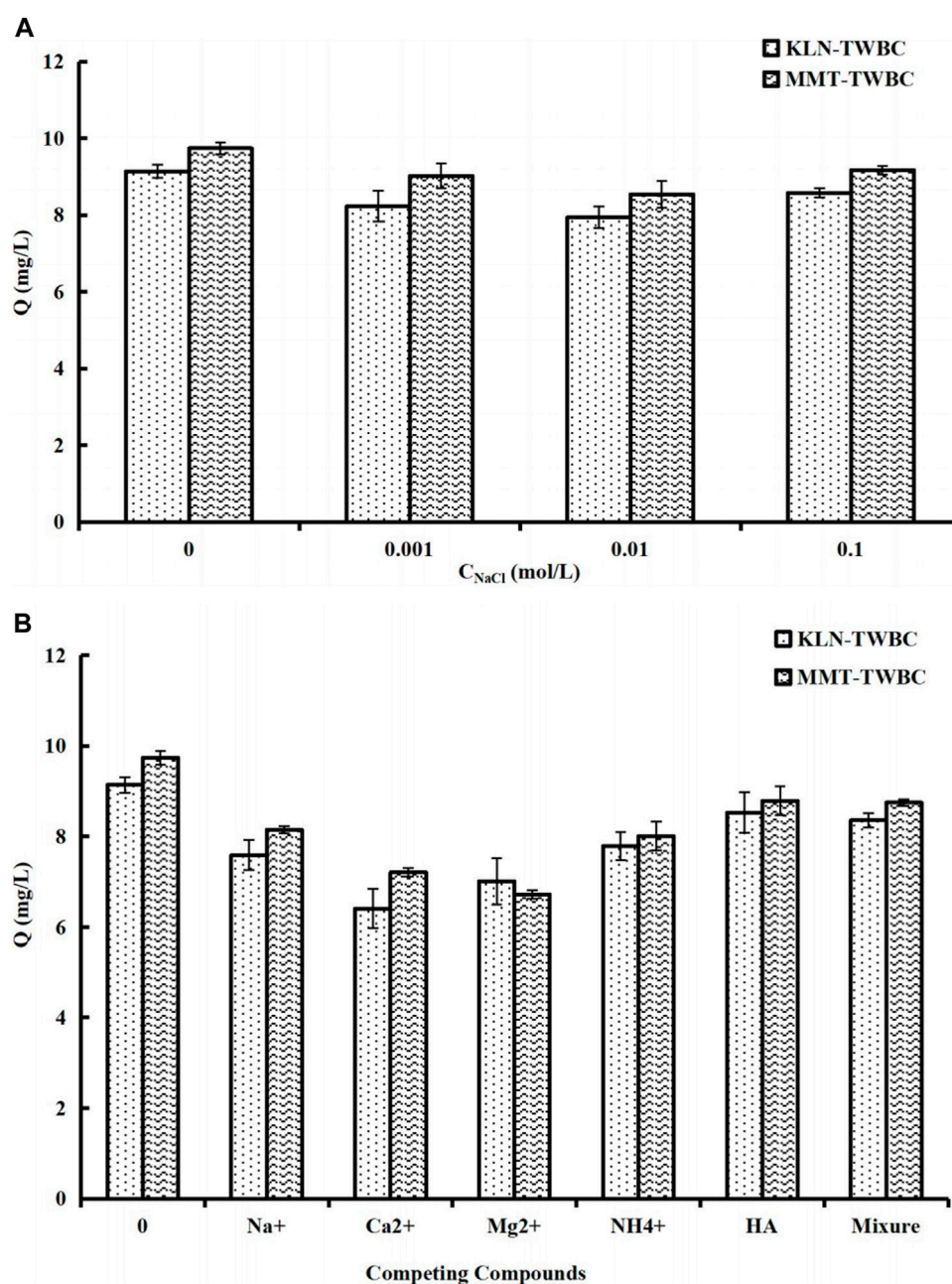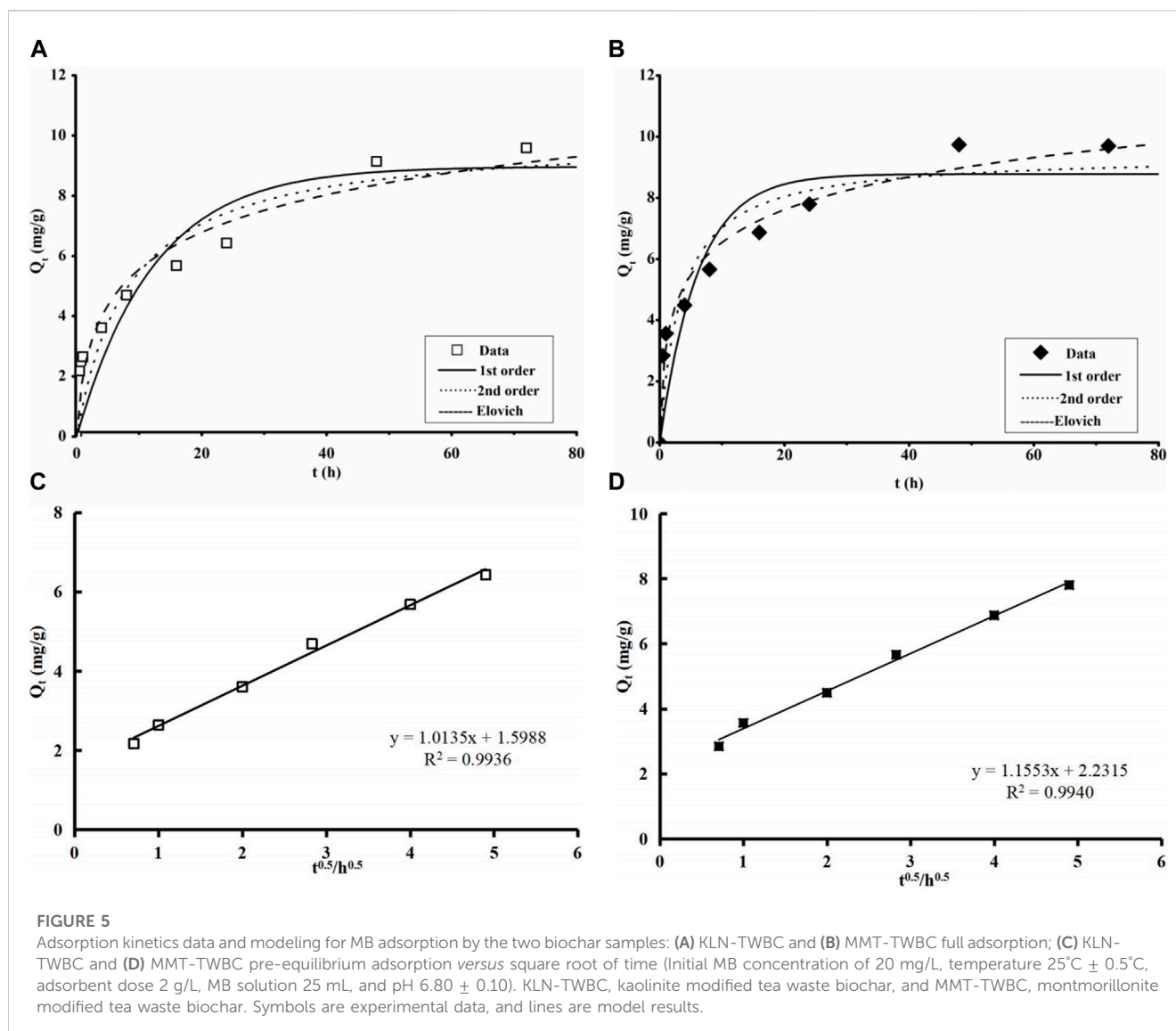
FIGURE 4
Effect of **(A)** ionic strength (IS) and **(B)** competing compounds on MB adsorption for KLN-TWBC and MMT-TWBC (Initial MB concentration of 20 mg/L, contact time 48 h, temperature 25°C $\pm$ 0.5°C, adsorbent dose 2 g/L, MB solution 25 mL, and pH 6.80 $\pm$ 0.10). KLN-TWBC, kaolinite modified tea waste biochar, and MMT-TWBC, montmorillonite modified tea waste biochar. Error bars represent the standard deviations of triplicate samples.

of KLN-TWBC and MMT-TWBC, the effects of IS and competing compounds were examined. As show in Figure 4A, the MB adsorption ability of both clay-biochars was best without any interference, and the lowest adsorption capacities of MB can be founded at the conditions of IS ranging from 0.001 to 0.01 mol/L conversely, indicating that low IS had an adverse effect on MB adsorption for both clay-biochars. There was not noticeable impact on MB adsorption as IS is over 0.01 mol/L, and the adsorption performance was comparable with that at the

condition without any interference, which may be attributed presumably to dimerization and hydrophobic effect of cationic dye at the IS over 0.01 mol/L (Qiu et al., 2009; Liu et al., 2018). Similar negative effects on MB adsorption also occurred in the experiment with competing compounds, though the HA did not exhibited obvious effect (Figure 4B). MB adsorption ability dramatically declined in the presence of competing compounds, particularly divalent ions (i.e., Ca^{2+} and Mg^{2+}). The results from the test with competing compounds

FIGURE 5
Adsorption kinetics data and modeling for MB adsorption by the two biochar samples: **(A)** KLN-TWBC and **(B)** MMT-TWBC full adsorption; **(C)** KLN-TWBC and **(D)** MMT-TWBC pre-equilibrium adsorption *versus* square root of time (Initial MB concentration of 20 mg/L, temperature 25°C ± 0.5°C, adsorbent dose 2 g/L, MB solution 25 mL, and pH 6.80 ± 0.10). KLN-TWBC, kaolinite modified tea waste biochar, and MMT-TWBC, montmorillonite modified tea waste biochar. Symbols are experimental data, and lines are model results.

indicated the key role of the cation exchange in governing the adsorption of MB onto both clay-biochars. Cation exchange is non-specific, and adsorption sits can be taken up by other competing compounds (i.e., positive ions), thus the reduction of MB adsorption can be explained by high CEC onto both clay-biochars due to the implanted KLN and MMT, as well as oxygenic functional groups on the surface of biochar. While the coexisting cations have adverse effects, the experimental results demonstrated that clay-TWBCs created in this work is still effective for MB adsorption, especially under low cation concentration conditions.

3.3 Adsorption kinetics and isotherm

To better recognize the processes controlling the adsorption of MB onto KLN-TWBC and MMT-TWBC, studies including both kinetics and isotherm were

conducted and adsorption models were applied. The data and models for MB adsorption by both clay-TWBCs are shown in Figures 5, 6.

3.3.1 Adsorption kinetics

Both clay-biochars exhibited similar trends in MB adsorption over the contact time. Briefly, the experiment data for the adsorption of MB onto KLN-TWBC and MMT-TWBC showed a rapid initial adsorption phase followed by a slow phase, with equilibrium reached after 24 h (Figures 5A, B). The rapid adsorption phase is mainly governed by physisorption, and chemisorption is the important force controlling the slow adsorption phase until reaching equilibrium. In Table 2, the best-fit parameters are shown, and the Elovich model fits the experimental data best with R^2 of 0.9572 for KLN-TWBC and 0.9765 for MMT-TWBC. Elovich model assumes that the chemisorptions participated in the process of pollutants adsorption onto the heterogeneous surfaces. Hence, the adsorption of MB onto both clay-bichars in this work
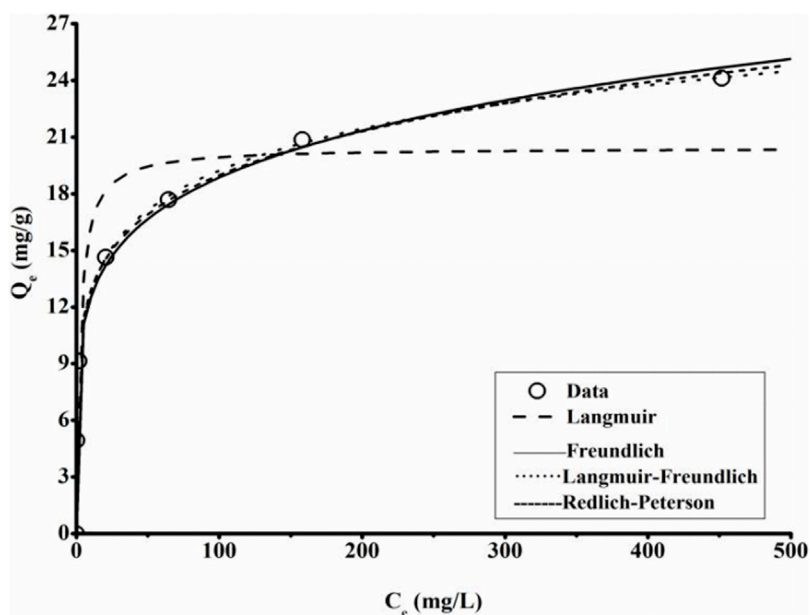
FIGURE 6
Adsorption isotherm data and modeling for MB adsorption by KLN–TWBC (Contact time 48 h, temperature 25°C ± 0.5°C, adsorbent dose 2 g/L, MB solution 25 mL, and pH 6.80 ± 0.10). KLN–TWBC, kaolinite modified tea waste biochar. Symbols are experimental data, and lines are model results.

TABLE 2 Best-fit models parameter of MB adsorption kinetics and isotherms.

		Parameter1	Parameter2	Parameter3	R^2
	Adsorption kinetics				
	First-order	$k_1 = 8.151 \times 10^{-2}$ h^{-1}	Qe = 8.968 mg/g		0.8595
	Second-order	$k_2 = 1.202 \times 10^{-2}$ g/(mg h)	Qe = 10.00 mg/g		0.9034
	Elovich	$\beta = 5.437 \times 10^{-1}$ g/mg	$\alpha = 3.584$ mg/(g h)		0.9572
KLN-TWBC	Adsorption isotherms				
	Langmuir	$K = 3.912 \times 10^{-1}$ L/mg	Q = 20.44 mg/g		0.8945
	Freundlich	$K_f = 8.291$ mg$^{(1-n)}$ L^n/g	$n = 1.785 \times 10^{-1}$		0.9973
	Langmuir-Freundlich	$K_{lf} = 1.704 \times 10^{-1}$ L^n/mg^n	Q = 55.08 mg/g	$n = 2.491 \times 10^{-1}$	0.9998
	Redlich-Peterson	$K_r = 1.871$ L/g $\times 10^2$ L/g	$a = 21.13$ L^n/mg^n	$n = 8.341 \times 10^{-1}$	0.9993
	Adsorption kinetics				
	First-order	$k_1 = 1.638 \times 10^{-1}$ h^{-1}	Qe = 8.780 mg/g		0.8314
	Second-order	$k_2 = 3.133 \times 10^{-2}$ g/(mg h)	Qe = 9.406 mg/g		0.9016
	Elovich	$\beta = 6.412$ g/mg $\times 10^{-1}$ g/mg	$\alpha = 10.21$ mg/(g h)		0.9765
MMT-TWBC	Adsorption isotherms				
	Langmuir	$K = 1.058$ L/mg	Q = 23.61 mg/g		0.8753
	Freundlich	$K_f = 11.18$ mg$^{(1-n)}$ L^n/g	$n = 1.558 \times 10^{-1}$		0.9573
	Langmuir-Freundlich	$K_{lf} = 2.216$ L^n/mg^n $\times 10^{-1}$ L^n/mg^n	Q = 58.58 mg/g	$n = 2.371 \times 10^{-1}$	0.9593
	Redlich-Peterson	$K_r = 1.845$ L/g $\times 10^2$ L/g	$a = 15.67$ L^n/mg^n	$n = 8.540 \times 10^{-1}$	0.9579

KLN-TWBC, kaolinite modified tea waste biochar; MMT-TWBC, montmorillonite modified tea waste biochar.

TABLE 3 Regeneration and cycle performance of KLN-TWBC and MMT-TWBC adsorbent.

Regeneration cycle	KLN-TWBC	MMT-TWBC
	Q^a mg/g	Q mg/g
0	24.12	27.89
1	21.38	23.94
2	18.46	23.39
3	20.02	25.20
4	20.46	22.65

[a]Q means the amount of MB adsorbed in each cycle.
KLN-TWBC, kaolinite modified tea waste biochar; MMT-TWBC, montmorillonite modified tea waste biochar.

could be governed by chemisorption *via* ion exchange or complexation. Furthermore, several previous studies regarding kinetic behavior have revealed that intraparticle diffusion is crucial to the adsorption process (Pignatello and Xing., 1995; Weerasooriya et al., 2007; Su et al., 2021; Zhou and Zhang, 2022). In this work, the adsorption of MB onto both clay-biochars also indicated diffusion limitation (Figures 5C, D). The pre-equilibrium (i.e., before 24) MB adsorption indicated a high linear dependency, more than 0.99 (R^2 = 0.9936 and 0.9940), on the square root of time (Figures 5C, D). Meanwhile, the straight line had a huge intercept of 1.599 and 2.24 mg/g, respectively, meaning that the surface adsorption made a contribution to the rate-limiting phase since the intercept reveals the film diffusion (Kalavathy et al., 2005; Yao et al., 2013b; Liu R. et al., 2019). The result suggests that both film and intraparticle diffusion mechanisms may play a key role in governing the rate-limiting of MB adsorption for both clay-biochars.

3.3.2 Adsorption isotherms

Previous studies have shown the maximum adsorption capacity of ~15 mg/g for KLN and ~55 mg/g for MMT (Ghosh and Bhattacharyya, 2002; Gurses et al., 2006). As listed in Table 2, the isotherm results revealed that the presence of KLN and MMT dramatically boosted the MB adsorption performance of both clay-biochars with a maximum MB adsorption capacity of more than 20 mg/g. The value was approximately one-fold that of TWBC (Figure 2B), and even higher than that of KLN itself and MMT-biochar synthesized using the conventional technology as well (Yao et al., 2014). Compared with other carbon adsorbents, such as activated carbons or engineering biochars prepared using conventional technologies, the MB adsorption ability of the clay-TWBC materials was lower (Carrier et al., 2012; Zhang et al., 2012; Liu S. et al., 2019; Huang et al., 2020; Yang L. et al., 2021). Thus, the clay treatment could be effectively used to promote MB adsorption ability of biochar prepared through the facile one-step technology. However, additional studies are still required to optimize the synthesis to improve its adsorption capacity.

The fitting models of both KLN-TWBC and MMT-TWBC were nearly identical and nearly all models reproduced good data (R^2 > 0.95), except for the Langmuir model (Figure 6). Table 2 lists a range of parameters of the isotherms models. For KLN-TWBC, Langmuir-Freundlich and Redlich-Peterson models presented better fitting performance than the other two (R^2 of 0.9998 and 0.9993,

respectively), while the slightly better fitting performance for MMT-TWBC was only Langmuir-Freundlich, with R^2 of 0.9593. Both Langmuir-Fredundlich and Redlich-Peterson models are usually used to described heterogeneous adsorption process. Also, Redlich-Peterson isotherm is a combined model including both Langmuir and Freundlich models, and has one more parameter than the Langmuir and Freundlich isotherms, resulting in better fitting. The good fit of the Redlich-Peterson isotherm can offer insight about the adsorption process. The "n" value in Redlich-Peterson was between 0 and 1. The closer the "n" value is to 1, the better Langmuir model can describe the adsorption process. As the "n" value is nearly 0, this reveals that data fitted with Freundlich model conversely. Therefore, findings shown that the interaction MB and clay-TWBCs could be impacted by both the Langmuir and Freundlich processes, and the adsorption of MB should be multilayer onto a heterogeneous surface, which is consistence with the characterization (Figure 1).

3.4 Regeneration and adsorption mechanisms

According to the previous result that KLN and MMT had successfully been implanted on the surface of TWBC through the facile one-step technology, the dominated mechanism responsible for the adsorption of MB onto both clay-bicoahrs could be explained by cation exchange. A generation experiment was conducted to further confirm the hypothesis, and to test the cyclic performance of KLN-TWBC and MMT-TWBC as adsorbents by carrying out multiple cycle adsorption experiments (Table 3). In the beginning, the MB adsorption capacity of KLN-TWBC and MMT-TWBC were 24.12 and 27.89 mg/g, respectively. After four recycles, MB adsorption confirmed that both clay-biochars were able to adsorb MB repeatedly with a relatively stable adsorption performance of approximately 20.08 and 23.80 mg/g, occupying more than 80% of the initial capacity, which indicated both clay-biochars had a potential of reusability for MB adsorption. In addition, based on the MB adsorption results from the high MB concentration discussed above, we found that TWBC from KLN-TWBC and MMT-TWBC accounted for 55.75% and 48.21% of MB adsorption. In comparison, KLN and MMT explained for the remaining 44.25% and 51.79% (Figure 2B). This result, combing with the

regeneration study, revealed that biochar itself (TWBC) and clays (KLN and MMT) can play a key role in governing MB adsorption with cation exchange and other mechanisms. Two reasons could explain the mechanisms responsible for cation exchange: 1) Both clays have the high CEC. The adsorption of MB onto KLN can be attributed to exchange reaction between MB and Al (III) and/or silanol group located on the surface of KLN, whereas the reaction occurs between MB and Al (III), Fe (III) and/or Ca (II) located in the interlayer of MMT (Ghosh and Bhattacharyya, 2002; Wang et al., 2008). 2) The high CEC was from TWBC due to relatively more O content of TWBC, since some of them are probably as oxygenic functional groups and usually exist on biochars' surface (Xue et al., 2012; Liu S. et al., 2019; Liu et al., 2020). In addition to cation exchange, biochar itself also can adsorb a small quantity of MB by the electrostatic attraction between the positive MB and the negatively charged biochars' surface, which might commonly be non-reversible.

4 Conclusion

A simple and environmental-friendly technology (with facile low-temperature in the presence of air) was developed to create engineered biochars from tea waste pretreated with clay, which made it possible to produce biochar-supported clay on a large scale. KLN- and MMT-biochar exhibited excellent MB adsorption capacity. However, a slight decline in MB adsorption ability occurred when the initial pH and IS are low, or competing compounds existed in MB solution. In addition, due to stability and cycle performance, both clay-biochars also can be regenerated and reused for removing MB. Findings indicate that the engineered biochars should be potentially served as a high-efficiency adsorbent to remove MB and even other cationic contaminants.

Data availability statement

The original contributions presented in the study are included in the article/Supplementary Material, further inquiries can be directed to the corresponding author.

Author contributions

RL: conceptualization, methodology, data curation, writing—original draft preparation, and funding acquisition. YCL: writing—review and editing. ZZ: software, methodology, and investigation. DL: methodology and investigation. JR: writing—review. YL: methodology and formal analysis. All authors have read and agreed to the published version of the manuscript.

Funding

Conflict of interest

The authors declare that the research was conducted in the absence of any commercial or financial relationships that could be construed as a potential conflict of interest.

Publisher's note

All claims expressed in this article are solely those of the authors and do not necessarily represent those of their affiliated organizations, or those of the publisher, the editors and the reviewers. Any product that may be evaluated in this article, or claim that may be made by its manufacturer, is not guaranteed or endorsed by the publisher.

Supplementary material

The Supplementary Material for this article can be found online at: https://www.frontiersin.org/articles/10.3389/fenvs.2023.1137284/full#supplementary-material

References

Basta, A. H., Fierro, V., Ei-Saied, H., and Celzard, A. (2009). 2-Steps KOH activation of rice straw: An efficient method for preparing high-performance activated carbons. *Bioresour. Technol.* 100, 3941–3947. doi:10.1016/j.biortech.2009.02.028

Basta, A. H., Fierro, V., Ei-Saied, H., and Celzard, A. (2011). Effect of deashing rice straws on their derived activated carbons produced by phosphoric acid activation. *Biomass. Bioenerg.* 35, 1954–1959. doi:10.1016/j.biombioe.2011.01.043

Carrier, M., Hardie, A. G., Uras, U., Gorgens, J., and Knoetze, J. (2012). Production of char from vacuum pyrolysis of South-African sugar cane bagasse and its characterization as activated carbon and biochar. *J. Anal. Appl. Pyrol.* 96, 24–32. doi:10.1016/j.jaap.2012.02.016

Chen, Z. L., Zhang, J. Q., Huang, L., Yuan, Z. H., Li, Z. J., and Liu, M. C. (2019). Removal of Cd and Pb with biochar made from dairy manure at low temperature. *J. Integr. Agr.* 18, 201–210. doi:10.1016/S2095-3119(18)61987-2

Ge, Q. L., Tian, Q., Moeen, M., and Wang, S. F. (2020). Facile synthesis of cauliflower leaves biochar at low temperature in the air atmosphere for Cu(II) and Pb(II) removal from water. *Materials* 13, 3163–3181. doi:10.3390/ma13143163

Ghosh, D., and Bhattacharyya, K, G. (2002). Adsorption of methylene blue on kaolinite. *Appl. Clay. Sci.* 20, 295–300. doi:10.1016/S0169-1317(01)00081-3

Gong, H. B., Zhao, L., Rui, X., Hu, J. W., and Zhu, N. W. (2022). A review of pristine and modified biochar immobilizing typical heavy metals in soil: Applications and challenges. *J. Hazard. Mat.* 432, 128668–128683. doi:10.1016/j.jhazmat.2022.128668

Gurses, A., Dogar, C., Yalcin, M., Acikyildiz, M., Bayrak, R., and Karaca, S. (2006). The adsorption kinetics of the cationic dye, methylene blue onto clay. *J. Hazard. Mat.* 131, 217–228. doi:10.1016/j.jhazmat.2005.09.036

Han, H. K., Wei, W., Jiang, Z. F., Lu, J. W., Zhu, J. J., and Xie, J. M. (2016). Removal of cationic dyes from aqueous solution by adsorption onto hydrophobic/hydrophilic silica aerogel. *Colloid. Surf. A* 509, 539–549. doi:10.1016/j.colsurfa.2016.09.056

Huang, C., Luo, M. N., Chen, F., He, J., and Wang, S. Y. (2020). Study on sorption characteristics of methylene blue by magnetic biochar derived from walnut shell. *Appl. Chem. Ind.* 49, 1956–1961+1965. doi:10.16581/j.cnki.issn1671-3206.20200611.045

Iriarte-Velasco, U., Chimeno-Alanis, N., Gonzalez-Marcos, M. P., and Alvarez-Uriarte, J. I. (2011). Relationship between thermodynamic data and adsorption/

desorption performance of acid and basic dyes onto activated carbons. *J. Chem. Eng. Data.* 56, 2100–2109. doi:10.1021/je1011345

Kalavathy, M. H., Karthikeyan, T., Rajgopal, S., and Miranda, L. R. (2005). Kinetic and isotherm studies of Cu (II) adsorption onto H₃PO₄-activated rubber wood sawdust. *J. Colloid. Interf. Sci.* 292, 354–362. doi:10.1016/j.jcis.2005.05.087

Kaya, A. (2004). Characterization of clay particle surfaces for contaminant sorption in soil barriers using flow microcalorimetry. *J. Environ. Eng-Asce.* 130, 918–921. doi:10.1061/(asce)0733-9372(2004)130:8(918)

Klika, Z., Pustkova, P., Dudova, M., Capkova, P., Klikova, C., and Grygar, T. M. (2011). The adsorption of methylene blue on montmorillonite from acid solutions. *Clay. Min.* 46, 461–471. doi:10.1180/claymin.2011.046.3.461

Liu, M., Che, Y., Wang, L., Zhao, Z., Zhang, Y., Wei, L., et al. (2019). Rice straw biochar and phosphorus inputs have more positive effects on the yield and nutrient uptake of Lolium multiflorum than arbuscular mycorrhizal fungi in acidic Cd-contaminated soils. *Chemosphere* 235, 32–39. doi:10.1016/j.chemosphere.2019.06.160

Liu, R., Li, S., Luo, X., Liu, D. D., and Zhang, H. (2021). Adsorption of inorganic contamination in aqueous solution with multifunctionalized biochar: A review. *Sci. Technol. Eng.* 21, 11455–11462.

Liu, R., Li, S., Zhang, H., Luo, X., and Yang, H. Y. (2019). Adsorption characterization of cationic and anionic dye from aqueous solution by HNO₃ modified biochar. *Technol. Water. Treat.* 45, 28–34. doi:10.16796/j.cnki.1000-3770.2019.03.006

Liu, R., Luo, X., Li, S., Zhang, H., and Liu, X. (2020). Biochar aging in soils and its influence on adsorption of heavy metals: A review. *Admin. Tech. Environ. Monit.* 32, 1–5. doi:10.19501/j.cnki.1006-2009.20200905.007

Liu, R., Zhang, H., Luo, X., and Yang, H. Y. (2018). Influence factors on adsorption of cationic and anionic dye from aqueous solution by HNO₃-modified biochar. *Sci. Technol. Eng.* 18, 332–338.

Liu, S., Li, J. H., Xu, S., Wang, M. Z., Zhang, Y. C., and Xue, X. H. (2019). A modified method for enhancing adsorption capability of banana pseudostem biochar towards methylene blue at low temperature. *Bioresour. Technol.* 282, 48–55. doi:10.1016/j.biortech.2019.02.092

Ma, Y. L., Xu, Z. R., Guo, T., and You, P. (2004). Adsorption of methylene blue on Cu(II)-Exchanged montmorillonite. *J. Colloid. Interf. Sci.* 280, 283–288. doi:10.1016/j.jcis.2004.08.044

Meng, J., Zhang, H. L., Cui, Z. H., Guo, H. P., Mašek, O., Sarkar, B., et al. (2022). Comparative study on the characteristics and environmental risk of potentially toxic elements in biochar obtained via pyrolysis of swine manure at lab and pilot scales. *Sci. Total. Environ.* 825, 153941. doi:10.1016/j.scitotenv.2022.153941

Mohan, D., Sarswat, A., Ok, Y. S., and Jr, C. U. P. (2014). Organic and inorganic contaminants removal from water with biochar, a renewable, low cost and sustainable adsorbent-a critical review. *Bioresour. Technol.* 160, 191–202. doi:10.1016/j.biortech.2014.01.120

Murray, H. H. (1991). Overview, clay mineral applications. *Appl. Clay. Sci.* 5, 379–395. doi:10.1016/0169-1317(91)90014-Z

Ngulube, T., Gumbo, J. R., Masindi, V., and Maity, A. (2017). An update on synthetic dyes adsorption onto clay based minerals: A state-of-art review. *J. Environ. Manage.* 191, 35–57. doi:10.1016/j.jenvman.2016.12.031

Pignatello, J. J., and Xing, B. (1995). Mechanisms of slow sorption of organic chemicals to natural particles. *Eniron. Sci. Technol.* 30, 1–11. doi:10.1021/es940683g

Qiu, Y. P., Zheng, Z. Z., Zhou, Z. L., and Shen, G. D. (2009). Effectiveness and mechanisms of dye adsorption on a straw-based biochar. *Bioresour. Technol.* 100, 5348–5351. doi:10.1016/j.biortech.2009.05.054

Simsir, H., Eltugral, N., and Karagoz, S. (2007). Hydrothermal carbonization for the preparation of hydrochars from glucose, cellulose, chitin, chitosan and wood chips via low-temperature and their characterization. *Bioresour. Technol.* 246, 82–87. doi:10.1016/j.biortech.2017.07.018

Sizmur, T., Fresno, T., Akgül, G., Frost, H., and Moreno-Jiménez, M. (2017). Biochar modification to enhance sorption of inorganics from water. *Bioresour. Technol.* 246, 34–47. doi:10.1016/j.biortech.2017.07.082

Su, L., Zhang, H. B., Cheng, H. Y., Zhang, G. S., Luo, Y., He, X. F., et al. (2021). Study on adsorption properties of biochar derived from spent auricularia substrate for cationic dyes. *China Environ. Sci.* 41, 693–703. doi:10.19674/j.cnki.issn1000-6923.2021.0080

Wang, D. Q., Guo, J. G., Wang, F. Y., and Zhang, H. F. (1996). A study on the occurrence of iron in montmorillonite. *Acta. Min. Sin.* 16, 62–65. doi:10.16461/j.cnki.1000-4734.1996.01.011

Wang, L., Zhang, j., and Wang, A. (2008). Removal of methylene blue from aqueous solution using chitosan-g-poly (acrylic acid)/montmorillonite superadsorbent nanocomposite. *Colloid Surf. A* 322, 47–53. doi:10.1016/j.colsurfa.2008.02.019

Weerasooriya, R., Tobschall, H. J., Seneviratne, W., and Bandara, A. (2007). Transition state kinetics of Hg(II) adsorption at gibbsite–water interface. *J. Hazard. Mat.* 147, 971–978. doi:10.1016/j.jhazmat.2007.01.134

Xue, Y. W., Gao, B., Yao, Y., Inyang, M., Zhang, M., Zimmerman, A. R., et al. (2012). Hydrogen peroxide modification enhances the ability of biochar (hydrochar) produced from hydrothermal carbonization of peanut hull to remove aqueous heavy metals: Batch and column tests. *Chem. Eng. J.* 200-202, 673–680. doi:10.1016/j.cej.2012.06.116

Yan, H., Zhang, W. X., Kan, X. W., Dong, L., Jiang, Z. W., Li, H. Z., et al. (2011). Sorption of methylene blue by carboxymethyl cellulose and reuse process in a secondary sorption. *Colloid Surf. A* 380, 143–151. doi:10.1016/j.colsurfa.2011.02.045

Yan, S. J., Hu, J. H., Liu, Z. W., Yuan, X. T., and Li, H. (2018). Experimental study on the effect of temperature and low oxygen conditions on pore structure of molding biochar. *Chem. Ind. Eng. Pro.* 37, 3100–3106. doi:10.16085/j.issn.1000-6613.2017-2103

Yang, J. H., Zhang, H. L., Liang, J. J., and Hu, Z. K. (2021). Adsorption of methylene blue by chitosan/magnetic durian biochar. *Environ. Sci. Technol.* 44, 7–12. doi:10.19672/j.cnki.1003-6504.18772.21.338

Yang, L., Fu, J., Wen, Z. W., Xia, R., Pan, G. X., and Yang, L. M. (2021). Preparation and structure characterization of six kinds of lwo temperature biochar. *J. Jilin Agr. Univ.* 43, 565–573. doi:10.13327/j.jjlau.2021.5153

Yao, Y., Gao, B., Chen, J. J., and Yang, L. Y. (2013b). Engineered biochar reclaiming phosphate from aqueous solutions: Mechanisms and potential application as a slow-release fertilizer. *Environ. Sci. Technol.* 47, 8700–8708. doi:10.1021/es4012977

Yao, Y., Gao, B., Chen, J. J., Zhang, M., Inyang, M., Li, Y. C., et al. (2013a). Engineered carbon (biochar) prepared by direct pyrolysis of Mg-accumulated tomato tissues: Characterization and phosphate removal potential. *Bioresour. Technol.* 138, 8–13. doi:10.1016/j.biortech.2013.03.057

Yao, Y., Gao, B., Fang, J., Zhang, M., Chen, H., Zhou, Y. M., et al. (2014). Characterization and environmental applications of clay-biochar composites. *Chem. Eng. J.* 242, 136–143. doi:10.1016/j.cej.2013.12.062

Yu, Q. Y. (2011). Advances in the treatment of printing and dyeing wastewater. *Ind. Saf. Environ. Prot.* 37, 41–43.

Zhang, M., Gao, B., Yao, Y., Xue, Y. W., and Inyang, M. (2012). Synthesis, characterization, and environmental implications of graphene-coated biochar. *Sci. Total. Environ.* 435, 567–572. doi:10.1016/j.scitotenv.2012.07.038

Zhao, G. G., Sun, J., Zhang, Y. B., Wang, H. B., and Wu, J. S. (2021). Research progess of advanced oxidation technology in treatment of printing and dyeing wastewater. *Appl. Chem. Ind.* 50, 2550–2554+2558. doi:10.16581/j.cnki.issn1671-3206.20210630.003

Zhao, T., Yao, Y., Li, D. R., Wu, F., Zhang, C. Z., and Gao, B. (2018). Facile low-temperature one-step synthesis of pomelo peel biochar under air atmosphere and its adsorption behaviors for Ag(I) and Pb (II). *Sci. Total. Environ.* 640-641, 73–79. doi:10.1016/j.scitotenv.2018.0.5.251

Zhou, R. J., and Zhang, M. (2022). Adsorption characteristics of heavy metal ions in water by water hyacinth biochar. *Saf. Environ. Eng.* 29, 168–177. doi:10.13578/j.cnki.issn.1671-1556.20210847

Zhuang, J., and Yu, G. R. (2022). Effects of surface coatings on electrochemical properties and contaminant sorption of clay minerals. *Chemsphere* 49, 619–628. doi:10.1016/S0045-6535(02)00332-6